Hindawi
Advances in Civil Engineering
Volume 2022, Article ID 1296288, 14 pages
https://doi.org/10.1155/2022/1296288

Research Article

Effect of Dry-Wet Cycles on Strength Properties and Microstructure of Lime-Metakaolin-Modified Soil

Xinming Li,[1] **Haoyang Zhang**,[1] **Yanrui Guo**,[1] **Song Yin**,[1] **and Kebin Ren**[2]

[1]*School of Civil Engineering and Architecture, Zhongyuan University of Technology, Zhengzhou, Henan 450007, China*
[2]*Henan Provincial Architectural Heritage Protection and Research Institute, Zhengzhou 450002, China*

Correspondence should be addressed to Xinming Li; xmli@zut.edu.cn and Haoyang Zhang; 858525595@qq.com

Received 25 April 2022; Accepted 15 July 2022; Published 29 September 2022

Academic Editor: Ramadhansyah Putra Jaya

To explore the feasibility of replacing natural hydraulic lime (NHL) with lime-metakaolin (L-MK) in the restoration of soil sites, the samples of L-MK-modified silty sand (hereinafter L-MK-modified soil) underwent 0, 5, 10, and 15 dry-wet cycles and were then tested for mass loss, unconfined compressive strength, and splitting tensile strength. Some samples were tested using XRD, TG and SEM microscopic tests to study the strength mechanism for L-MK- and NHL-modified soil. The results showed that the mass loss ratios of the L-MK- and NHL-modified soils after 15 dry-wet cycles were within 2%. The compressive and tensile strengths of the L-MK-modified soil decreased with more dry-wet cycles, but the tensile strength decreased sharply initially and then to be stable after five dry-wet cycles. The attenuation characteristics were different obviously for the failure mode of compressive and tensile strength and the unevenness of the specimen caused by dry-wet cycles. The compressive and tensile strengths of L-MK-modified soil were significantly higher than those of NHL-modified soil after the same dry-wet cycle, and the decreased range of compressive and tensile strength was smaller than that of NHL-modified soil. The strength formation and attenuation characteristics of L-MK-modified soil are closely related to the influence of dry-wet cycles on the hydration products (e.g., CSH and C_4AH_{13}) generated by hydration reaction. The mix proportion of 6% L + 4% MK can effectively replace 8% and 10% NHL to protect soil sites.

1. Introduction

Soil sites are cultural heritages with historical, artistic, and scientific value and constructed with soil as the main material. However, soil sites are damaged continuously in many aspects and exhibit many disease symptoms (i.e., basal deterioration and collapse) for the influences of meteorological, geological, and human [1]. Climatic conditions (i.e., dry-wet cycles) are considered to be highly damaging to infrastructure such as soil sites. For example, heavy rain occurs frequently in summer in the Central Plains of China, and the soil sites across this region are mostly rammed with silty soil or silty sand with strong water sensitivity [2]. They are prone to erosion, cracking, and even collapse under the repeated dry-wet effects [2]. Based on years of practical experience in protecting soil sites, it is concluded that the reasonable selection of restoration materials is the key to implementing preventive protection of soil sites. Therefore, it is very important to study the restoration materials of soil sites for slowing their damage and extending their effective preservation period.

According to the principle of minimum intervention in the protection of cultural relics, traditional restoration materials should be used as far as possible. At present, the materials applied to the restoration of soil sites mainly include inorganic materials such as lime [3], cement [4], and hydraulic lime [5]. Lime is an air-hardening material whose mechanical properties are unstable in water environments, which leads to the adverse situation of repeated repair and destruction of soil sites [6]. Although cement is characterized by hydraulicity and higher early strength, it is not proper for the problems of alkali return, uncoordinated strength, and deformation during its combination with the soil site [7]. Hydraulic lime since the 20th century was

developed and used in Europe and the United States and other countries, because of its moderate mechanical strength, proper water and air permeabilities, good compatibility with protected buildings, and strong resistance to wind and rain erosion and repeated changes in temperature and humidity [8–10]. However, it is limited by dependence on imports and high prices in China. Studies have shown that in the presence of water, the main active component of metakaolin (MK), i.e., anhydrous aluminum silicate ($SiO_2{\cdot}2Al_2O_3$), can react with the calcium hydroxide ($Ca(OH)_2$) in lime to form a hydrated product similar to the strength of cement [11, 12]. Lime and MK are common natural mineral materials in China with the advantages of a wide source of raw materials and low cost. Therefore, based on lime and MK, developing inorganic materials to replace natural hydraulic lime (NHL) is very important and proper for improving the protection level of Chinese soil sites and reducing the cost of protecting cultural relics.

Durability is a key feature of restoration materials for soil sites and is defined as the ability of a material to retain its stability and integrity and maintain adequate long-term residual strength to provide sufficient resistance to climatic conditions. Furthermore, dry-wet cycles are an important method for evaluating how water change influences the mechanical properties and microstructure of soil sites in the natural environment. Wang et al. [13] and Consoli et al. [14] compared the mechanical properties of lime-cured expansive soil and clay before and after dry-wet cycles and found that lime could effectively improve the resistance of soil to dry-wet cycles. However, the study by Yan et al. [15] of lime-improved loess found that its unconfined compressive strength (UCS) decreased sharply after two dry-wet cycles, and the strength loss was 29% after 10 dry-wet cycles. Aldaood et al. [16] conducted compressive strength and P-wave velocity tests of lime-improved gypsum soil under dry-wet cycles and found that the effect of lime improvement was unclear. Pavía and Treacy [17] evaluated the durability of lime mortar and weak hydraulic lime (NHL2) mortar by means of water migration characteristics, which showed that (i) lime mortar was more durable than NHL2 and (ii) NHL2 mortar had a higher risk of decomposition particles. Song al. [18] considered the durability of lime mortar to be poor and its strength growth rate to be slow, thereby limiting its engineering applications. Kalagri et al. [19] evaluated the durability of mortar by establishing empirical formulas for predicting its compressive and flexural strengths, and they concluded that the mechanical strength of hydraulic lime (NHL5) was around three times that of lime mortar and cement mortar. Forster and Carter [20] concluded that the content and grade of hydraulic lime affect its durability in building repair. By mixing MK and NHL at a ratio of 1 : 1, Sepulcre Aguilar and Hernández-Olivares [21] found that the durability and mechanical resistance of MK-NHL mortar were better than those of pure lime mortar and pure water-hard lime mortar.

As can be seen, the mechanical properties of lime and NHL-modified soil are quite different from the change rule of durability index such as dry-wet (D-W) cycles, and the variation law of mechanical properties is greatly related to the dry-wet cycle method, the soil properties of the substrate, and the mixing ratio. The influence of D-W on hydration products such as CSH and C_4AH_{13} generated by $Ca(OH)_2$ and SiO_2 and Al_2O_3 is not clear. Therefore, to provide material support and a theoretical basis for restoring soil sites, it is necessary to study the dry-wet cycle effect and microscopic mechanism of the mechanical properties of L-MK- and NHL-modified soil under specific substrate and environmental impact conditions.

In this study, dry-wet cycle effects for L-MK- and NHL-modified silty sand are investigated in line with the occurrence environment of soil sites. Samples with different mixture proportions under 0, 5, 10, and 15 dry-wet cycles are subjected to mass loss, UCS, and splitting tensile strength (STS) tests, and some representative samples are chosen for X-ray diffraction (XRD) analysis, differential scanning calorimetry and thermogravimetric analysis (DSC-TGA), scanning electron microscopy (SEM), and other microscopic tests to explore the correlation between the mechanical properties and microstructure characteristics of modified soil under dry-wet conditions. Finally, the feasibility of replacing NHL with L-MK for modified silty sand is explored and analyzed.

2. Materials and Test Methods

2.1. Raw Materials and Sample Preparation. The raw materials for the tests were silty sand, lime, MK, and NHL. The physical photographs of materials are shown in Figure 1, and the XRD test results are shown in Figure 2. The silty sand used in the tests was from the scattered soil of the Yuanling ancient soil site in the city of Zhengzhou in Henan Province; its main mineral composition was silica (SiO_2) accounting for 67.89%, followed by alumina (Al_2O_3) accounting for 11.58%. Its basic physical properties are given in Table 1. The lime and MK were provided by local Chinese company. The main mineral phases of lime were calcium hydroxide ($Ca(OH)_2$) and a small amount of calcium carbonate ($CaCO_3$). The 28d pozzolanic activity index of MK was 122%, and its mineral phases were amorphous aluminum silicate ($Al_2(Si_2O_5)(OH)_4$) with a small amount of SiO_2 and kaolinite. The main mineral phases of NHL were calcium silicate (C_2S), $CaCO_3$, $Ca(OH)_2$, and quartz. The chemical compositions of the four materials were determined by X-ray fluorescence, and the results are given in Table 2.

Banzibaganye et al. [22] found that the optimal content of lime in lime-improved silt soil is 6–8%. Combined with the relevant requirements of 10% lime + 90% soil, 20% lime + 80% soil, and 30% lime + 70% soil (in volume) commonly used in the protection of ancient buildings, three values of the lime mixing ratio (6%, 8%, and 10% in weight) and three values of the MK mixing ratio (4%, 8%, and 12% in weight) were selected to prepare L-MK-modified soil samples. The modified soil samples with 8% and 10% NHL were prepared for comparison. Samples were made in a cylindrical mold ($d = 50$ mm, $h = 50$ mm) with respective w_{op}, and the modified soil sample was remolded with the degree of sample compaction of 95% and then cured in a

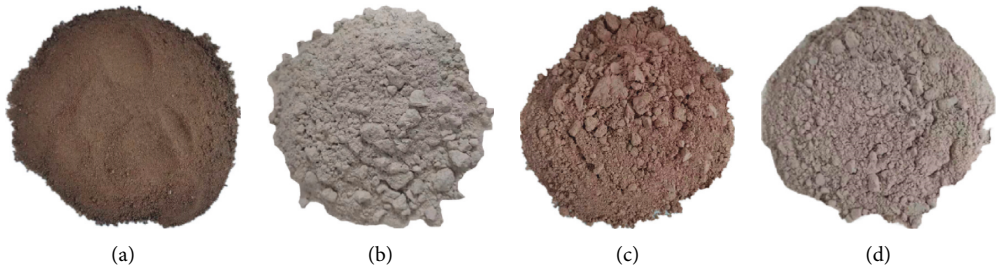

Figure 1: Test of raw materials. (a) Silty sand. (b) Lime. (c) MK. (d) NHL.

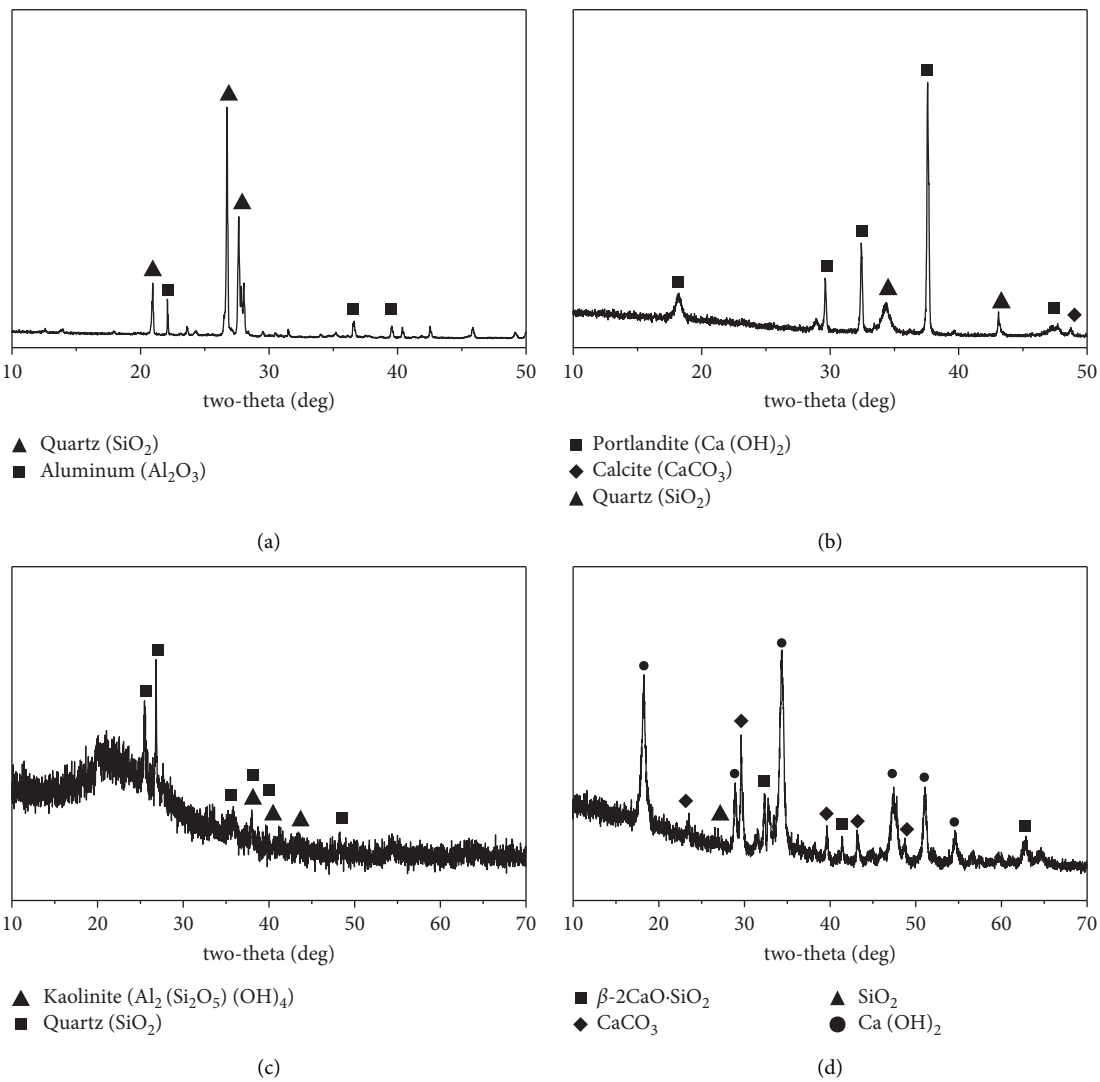

Figure 2: X-ray diffraction patterns (10~50°/10~70°) of silty sand soil (a), lime (b),metakaolin (c), and hydraulic lime (d).

Table 1: Basic properties of silty soil.

Optimal moisture content (%)	Max dry density (g/cm^3)	Liquid limit (%)	Plastic limit (%)	Plasticity index	Particle composition (%)		
					Sand (0.075~2 mm)	Silt (0.075~0.005 mm)	Clay (<0.005 mm)
9.3	1.96	19.2	8.22	10.98	65.66	32.48	1.86

Table 2: Main components of silty soil, lime, metakaolin, and hydraulic lime.

Materials	SiO_2	CaO	Fe_2O_3	TiO_2	Al_2O_3	K_2O	MgO	SO_3	Others
Silty soil	67.89	3.04	5.97	2.86	11.58	1.75	2.82	0.46	2.63
MK	49.73	1.72	2.23	1.56	41.18	0.17	0.13	0.09	3.19
NHL	13.33	75.36	1.60	0.14	2.62	0.99	2.16	0.67	3.13
Lime	1.01	95.60	0.21	—	1.55	—	0.16	0.06	2.12

curing chamber for 28 d under standard conditions (20 ± 2°C and 95 ± 2% relative humidity).

2.2. Dry-Wet Cycle Test Method. Ren et al. [23] monitored the moisture content of typical soil sites in the central China. It was found that the moisture content of silty soil or silty sand sites was the lowest in January (w = 3.6–7.8%) and the highest in September (w = 20.0%). Considering the influence of extreme climatic conditions, the drying temperature was taken as 50°C to restore the climatic conditions of the soil site to the maximum extent [24]. The specific test steps were as follows. A sample cured for 28d was placed in a drying oven at a constant temperature of 50°C for 2d to achieve a shrinkage-stable moisture content state (w = 5%), which was a dehumidifying process. The sample was then placed on a permeable stone, adding distilled water at 20 ± 2°C, and the water surface is kept 2.5 cm above the top of the sample. After adding water, let the sample soak in water for 12 hours, which was a humidifying process. It took 60 h to complete one dry-wet cycle, and 15 cycles were carried out. Figure 3 shows changes in the moisture content during the dry-wet cycles. For the convenience of expression, D-W is used to represent the dry-wet cycle process; e.g., "D-W = 5" means five dry-wet cycles. The unconfined compression strength (UCS) and splitting tensile strength (STS) tests were carried out on the specimens after 0, 5, 10, and 15 dry-wet cycles, and the microscopic test was carried out on the samples after failure.

2.3. UCS and STS Tests. The unconfined compression strength (UCS) and splitting tensile strength (STS) tests were conducted using a California bearing ratio tester at an axial strain rate of 2%/min. Furthermore, six parallel samples were prepared to improve the test reliability, and the average value was taken as the test result. The evaluation was carried out according to the national standards GB/T 50123–1999, ASTM D1883-99, and ASTM D5102-96.

2.4. Microscopic Test Method. The main objectives of the micro-structural investigations were to (i) determine the changes in the silty sand due to the L-MK treatment and dry-wet cycles and (ii) detect the formation of hydration products. XRD, DSC-TGA, and SEM were used to test the composition, content, and morphology of the hydration products of L-MK- and NHL-modified soil.

2.4.1. XRD Test. The 50 g samples under zero, five, 10, and 15 dry-wet cycles were crushed into powder after vacuum drying and then passed through a 0.15 mm sieve until there was no obvious granularity. Using a Bruker D8 Advance (40 kV/40 mA) X-ray diffractometer under constant step length (0.02°) and rate (8°/min) and within a test range of 2θ of 5–80°, the mineral phase composition of a sample for each ratio was determined under different dry-wet cycles.

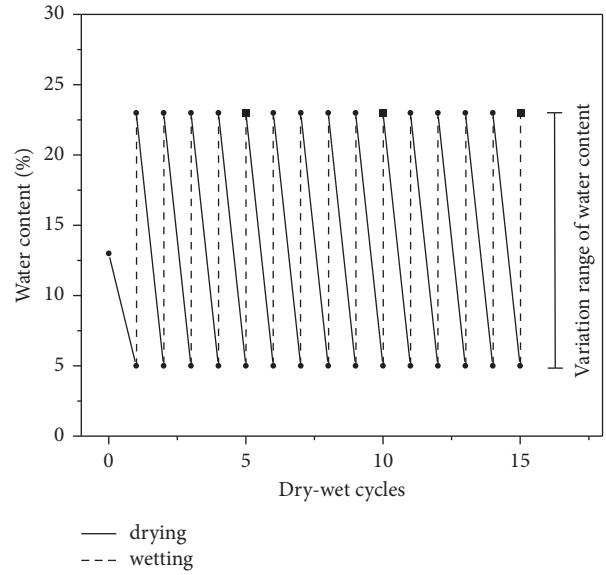

Figure 3: Changes in moisture content of sample during dry-wet cycle.

2.4.2. DSC-TGA Test. An STA 499 F5 synchronous thermal analyzer (DSC/DTA-TG) was used for the comprehensive DSC-TG analysis of the samples under different dry-wet cycles. The sample disposal method was the same as that in Section 2.4.1. To ensure better stability of the test results, the instrument for the TG and DSC test was started three hours in advance, and nitrogen (N_2) with an output pressure of 0.04 MPa was used to protect the samples. The test was carried out at a heating rate of 20°C/min, and the temperature range was 0–1000°C.

2.4.3. Micromorphology Observations. Fresh sample section slices with an approximate size of 1 cm^2 were taken for each ratio and cooled in liquid nitrogen at −190°C. After vacuuming for 24 h, the water in the samples was completely sublimated to the dry state. The morphology of the samples was observed by SEM (SU-8010).

3. Test Results

3.1. Mass Loss Test. Each sample was weighed after dry-wet cycle. The mass difference in a sample between consecutive

dry-wet cycles was not obvious, and the mass changes in samples after 15 dry-wet cycles are summarized instead in Figure 4.

Figure 4 shows the changes in sample mass after the dry-wet cycles. It can be concluded that the mass of each sample decreased gradually with more dry-wet cycles under different mixing ratios. For example, the mass of soil modified by 6% + 8% MK decreased from 205.06 g initially to 201.27 g after 15 dry-wet cycles, and the mass loss ratio was 1.45%. The mass of soil modified by 10% NHL decreased from 203.21 g initially to 202.3 g after 15 dry-wet cycles, and the mass loss ratio was 0.45%. The mass loss ratio of L-MK-modified soil is slightly larger than that of NHL-modified soil, but the overall loss ratio is less than 2%, which meets the requirements of the ASTM standard for the maximum allowable mass loss of silty soil under dry-wet cycles [25]. In addition, with constant lime content but increasing MK content, the mass loss of L-MK-modified soil decreases.

When the lime content is 8% and the MK content increased from 4% to 12%, the mass loss of the sample decreases from 1.98% to 1.15% after 15 dry-wet cycles. The analysis shows that with increasing MK content, the content of hydration products involved in the pozzolanic reaction increases gradually, forming cementitious materials and filling the soil pores. The soil particles are connected and wrapped around the periphery of the aggregates to form a stable structure, which enhances the cementation among soil particles and maintains the integrity of the soil structure. The mass loss of L-MK-modified soil was reduced.

3.2. UCS Test

3.2.1. Axial Stress-Strain Curve. Figure 5 shows the stress-strain curves of L-MK- and NHL-modified soils under different dry-wet cycles. Because the stress-strain curves of L-MK-modified soil with different mixing ratios are similar, only the test results of L-MK-modified soil with 8% lime are given for illustration. Figure 5 shows that the stress-strain curves of L-MK-modified soil before and after dry-wet cycles have obvious peak points as the strain-softening type. The peak stress of NHL-modified soil is more obvious without dry-wet cycles, but the softening characteristics weaken gradually under their action and are not obvious after 15 dry-wet cycles.

The strain corresponding to the peak stress in the stress-strain curve is defined as the failure strain ε_f. Compared with that before dry-wet cycles, the peak strain ε_f of the L-MK- and NHL-modified soils decreased with more dry-wet cycles. For example, after 5, 10, and 15 dry-wet cycles for soil modified by 8% L + 8% MK, ε_f decreased from 3.50% under no dry-wet cycles to 3.33%, 3.17%, and 3.00%, respectively. The deformation characteristics or capacity of soil can be measured by its failure strain. It can be concluded that the ability of soil to resist external load differs under dry-wet cycles, and eventually, the soil toughness is weakened [26].

3.2.2. UCS. When the stress-strain curve has a peak value, the corresponding strength is compressive strength. When the stress-strain curve has no peak or the peak is not obvious, the strength corresponding to an axial strain of 15% is compressive strength. The relationship between the compressive strength of L-MK- and NHL-modified soil and the number of dry-wet cycles is shown in Figure 6.

Figure 6 shows that the compressive strength of the L-MK- and NHL-modified soils decreased with more dry-wet cycles, but the L-MK-modified soil showed better resistance to dry-wet cycles. The attenuation range of the compressive strength of the L-MK-modified soil was 32.43–55.06%. For example, the compressive strength of soil modified by 8% L + 4% MK decreased from 5.06 MPa before any dry-wet cycles to 2.33 MPa after 15 dry-wet cycles, with a reduction of 53.95%. The compressive strength of soil modified by 8% and 10% NHL decreased by 87.96% and 90.82%, respectively, after 15 dry-wet cycles with the strength of only 0.49 MPa and 0.47 MPa. It can be concluded that after 15 dry-wet cycles, the compressive strength of the L-MK-modified soil was significantly higher than that of the NHL-modified soil, and the attenuation of the compressive strength of the L-MK-modified soil was significantly lower than that of the NHL-modified soil.

With constant lime content but increasing MK content, the attenuation of the compressive strength of the soil samples decreased. For example, when the lime content was 8% and the MK content increased from 4% to 12%, the compressive strength attenuation decreased from 53.95% to 37.07%. When the MK content was 4% and the lime content increased from 6% to 10%, the compressive strength attenuation decreased from 55.06% to 51.98%. The change in MK content is greater than that of lime content in improving soil mechanics. This indicates that with the incorporation of MK, the active component $SiO_2{\cdot}2Al_2O_3$ reacts with $Ca(OH)_2$ in lime to generate C-S(A)-H and other hydration products, thereby inhibiting the attenuation of strength by the dry-wet cycles. However, the hydration garnet formed by the reaction of α-Al_2O_3 with the high content of MK will have a negative impact on the mechanical strength of the soil [27]. Therefore, it is necessary to determine the content of MK reasonably in the restoration of soil sites, that is, to select a low content on the basis of meeting the requirements of stress and deformation.

Figure 6 also shows that the compressive strength of the L-MK-modified soil was still decreasing slowly after 15 dry-wet cycles, while the strength of the NHL-modified soil was basically stable after five dry-wet cycles. In the UCS test, the specimen was subjected to the hoop effect of the upper and lower loading steel plates, and the failure mode was mostly conical failure in the form of the upper and lower two cones, as shown in Figure 7(c). Although the specimen was subjected to uniaxial compression, the internal force field distribution was extremely uneven [28]. The area near the sample's surface was stretched horizontally. When the horizontal elongation strain exceeded the ultimate tensile strain of the soil, vertical cracks began to appear on the surface, as shown in Figure 7(b). At this time, the middle area of the specimen was under triaxial compression. Although the compression area and horizontal constraint force were decreasing, the soil could still withstand the pressure, and the main source of the compressive strength of the sample was the central area of the soil, as shown in

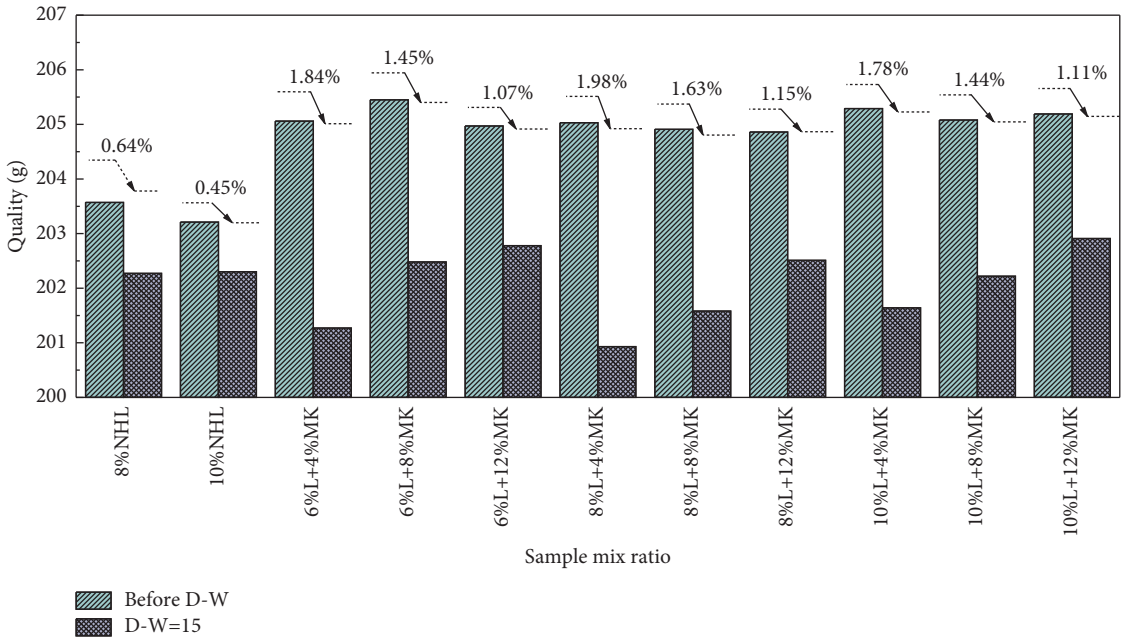

Figure 4: Changes in sample quality before and after dry-wet cycles.

Figure 7(a). That is to say, the smaller the influence of dry-wet cycles on the central region, the larger the volume range without external water damage, and the higher the UCS of the samples. This shows that with more dry-wet cycles, their influence on the central region of an L-MK-modified soil sample deepened gradually from the outside to the inside, resulting in a slow decrease in its strength. After five dry-wet cycles, the NHL-modified soil was seriously affected by them, resulting in a significant attenuation of its strength. This indicates that L-MK-modified soil has better resistance to dry-wet cycles.

3.3. STS. Figure 8 shows the relationship between the tensile strength of L-MK- and NHL-modified soils and the number of dry-wet cycles. It can be found that the tensile strength of the L-MK- and NHL-modified soils decreased with more dry-wet cycles. The tensile strength attenuation of the L-MK-modified soil after 15 dry-wet cycles was lower than that of the NHL-modified soil, and the absolute value of the tensile strength was between two and five times that of the NHL-modified soil under the same dry-wet cycles. When the number of dry-wet cycles was increased from zero to 15, the tensile strength of soil modified by 8% L + 4% MK decreased from 0.6 MPa to 0.25 MPa, and the attenuation was 58.33%. The tensile strength of soil modified by 8% and 10% NHL decreased from 0.58 MPa and 0.73 MPa, respectively, to 0.09 MPa after 15 dry-wet cycles, and the attenuation range was 84.48% and 87.67%, respectively.

The attenuation range of the tensile strength of the L-MK-modified soil was concentrated mainly in the first five dry-wet cycles, and the attenuation process exhibited a steep drop after five dry-wet cycles. For example, the tensile strength of soil modified by 8% L + 8% MK decreased by 47.14% after five dry-wet cycles and continued to increase to 7.15% after 15 dry-wet cycles. The splitting tensile failure mode of the samples in Figure 9(b) shows that the failure mode was typical splitting failure with a main crack; that is, the sample splits into two parts from the middle. The force field distribution of STS is clear, and there are only horizontal tensile stress and vertical compressive stress on the splitting surface. When the water-weakened part reached a certain depth from the deep center of the sample surface, it entered the area of maximum tensile stress (the core part represented by the virtual cylinder in Figure 9(a)) [27]. Unlike the UCS, the STS reflects the tensile strength of the outer part of the sample weakened by water, that is, the outer area of the sample that is strongly affected by the dry-wet cycles, which determines the tensile strength, and the central area is no longer the decisive factor of the ultimate load. Figure 6 shows that the attenuation of the compressive strength had no obvious piecewise process, and there was still a slow downward trend after 15 dry-wet cycles. For example, the attenuation of the compressive strength of soil modified by 8% L + 8% MK between 0 and 5 dry-wet cycles was 27.73%, and the attenuation between 5 and 15 dry-wet cycles was 22.22%.

From the above results for tensile and compressive resistance, it can be concluded that in the process of the dry-wet cycle test, water infiltrated the sample from the outside to the inside, and the outer structure of the soil was first affected by the dry-wet cycles. With more test time, the volume range of the central area of the soil affected by the dry-wet cycles continued to increase. However, before the central area of the soil was completely destroyed by the dry-wet effect, the outer structure of the soil had been destroyed. The internal and external heterogeneity of the dry-wet cycles caused the difference in the attenuation laws of the tensile and compressive strengths.

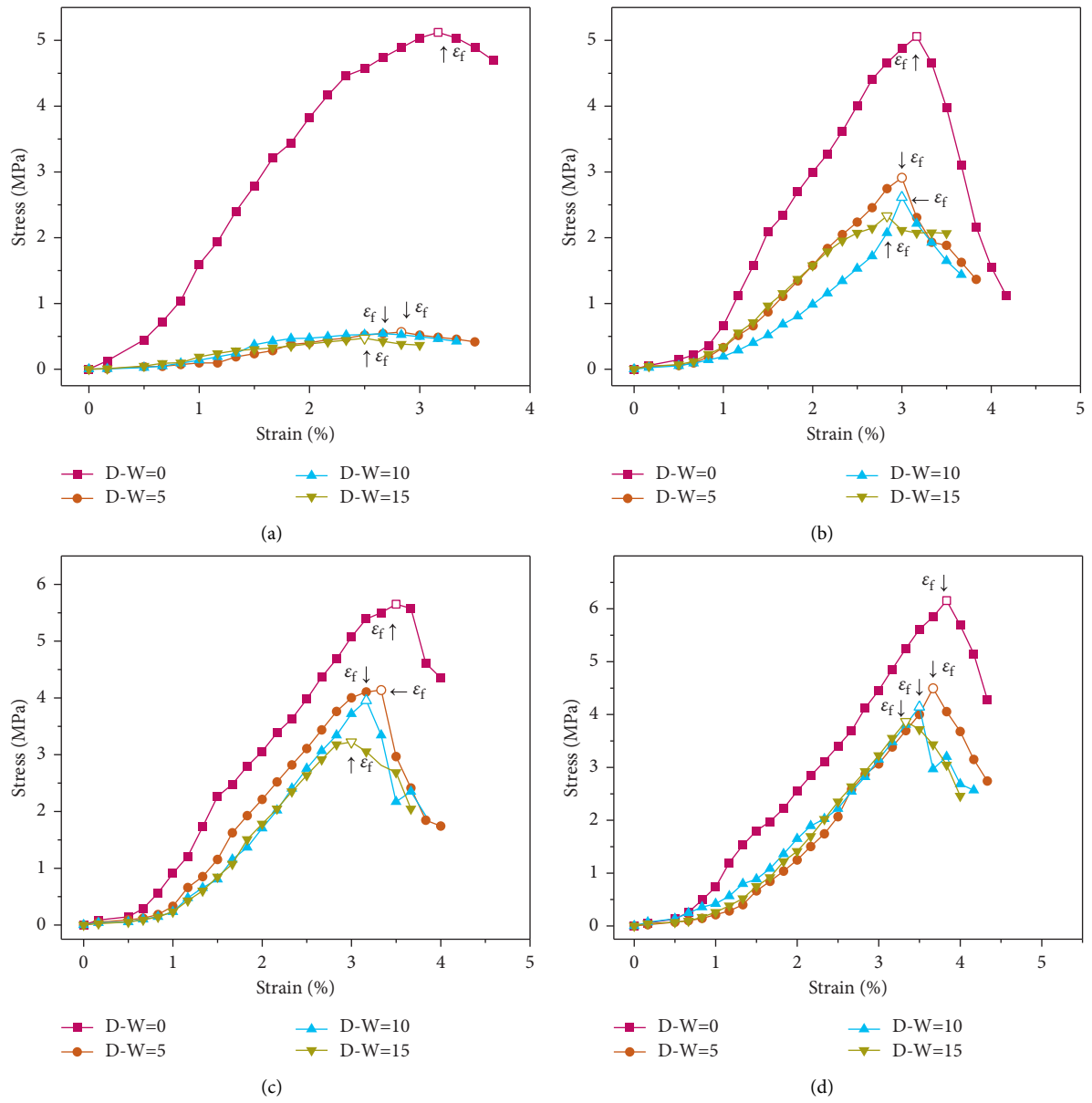

Figure 5: Stress-strain curve of sample. (a) 10% NHL. (b) 8% L + 4% MK. (c) 8% L + 8% MK. (d) 8% L + 12% MK.

3.4. Relationship between UCS and STS. Figure 10 shows the relationship between the compressive and tensile strengths of the L-MK- and NHL-modified soil, where R^2 is the goodness-of-fit index (proportional to the data accuracy and approximately unity in most situations). Figure 10 shows that the fitting parameter for the compressive and tensile strengths of the L-MK-modified soil before any dry-wet cycles was 8.04; that is, the compressive strength was 8.04 times the tensile strength. However, the fitting parameter increased to 9.54 after 15 dry-wet cycles. As shown, the attenuation range of the UCS of the soil was slightly larger than that of the STS, which is consistent with the attenuation results for the compressive and tensile strengths (Figures 6 and 8). It is also verified that the brittleness of the soil decreased, the plasticity increased, and the corresponding failure form changed from brittle failure to plastic failure under dry-wet conditions. The fitting parameter for the NHL-modified soil showed the opposite change rule; that is, it decreased from 7.02 before any dry-wet cycles to 5.44 after 15 dry-wet cycles, but it was lower than that of the L-MK-modified soil. This is consistent with the variation of the stress-strain curve for the NHL-modified soil in Figure 5(a).

4. Micromechanism

4.1. XRD Test. Figure 11 shows the XRD measurements of the L-MK- and NHL-modified soils before dry-wet cycles and after 15 dry-wet cycles in the range of 20–40°. Figure 11 shows that, except for $Ca(OH)_2$ in lime and the quartz contained in the soil itself, the pozzolanic reaction of L-MK produced hydration products similar to those of NHL-modified soils, mainly including amorphous calcium silicate hydrate ($CaO\text{-}SiO_2\text{-}H_2O$, CSH) and tetracalcium aluminate hydrate ($4CaO{\cdot}Al_2O_3{\cdot}13H_2O$, C_4AH_{13}). This is the hydration

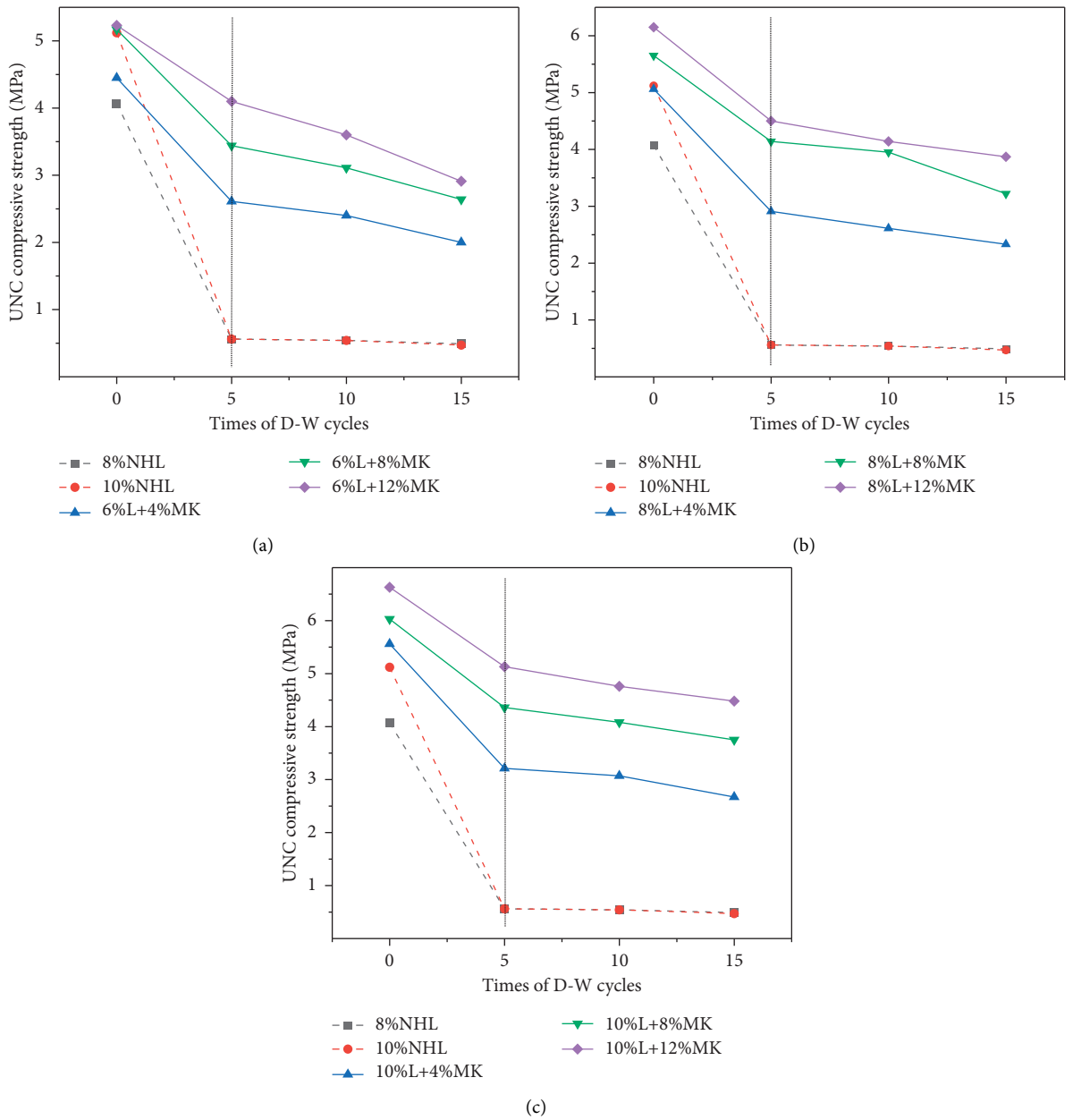

Figure 6: Relationship between the compressive strength of L-MK- and NHL-modified soils and the number of dry-wet cycles. (a) 6% L-MK and NHL. (b) 8% L-MK and NHL. (c) 10% L-MK and NHL.

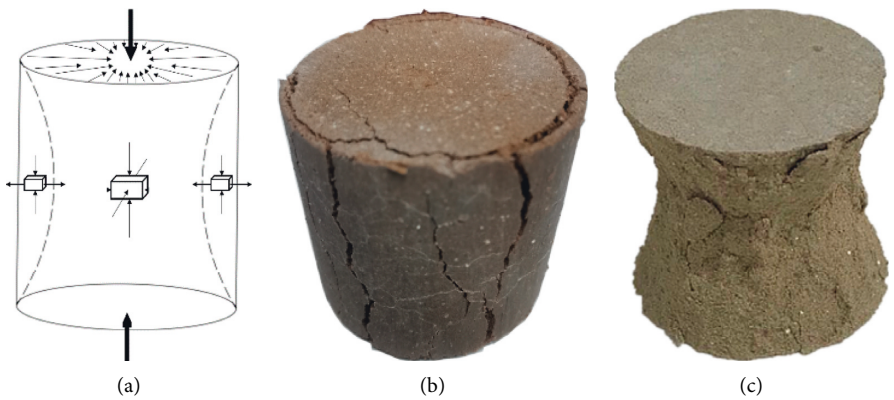

Figure 7: UNC compression failure mode and morphology. (a) Stress state. (b) Failure process. (c) Failure mode.

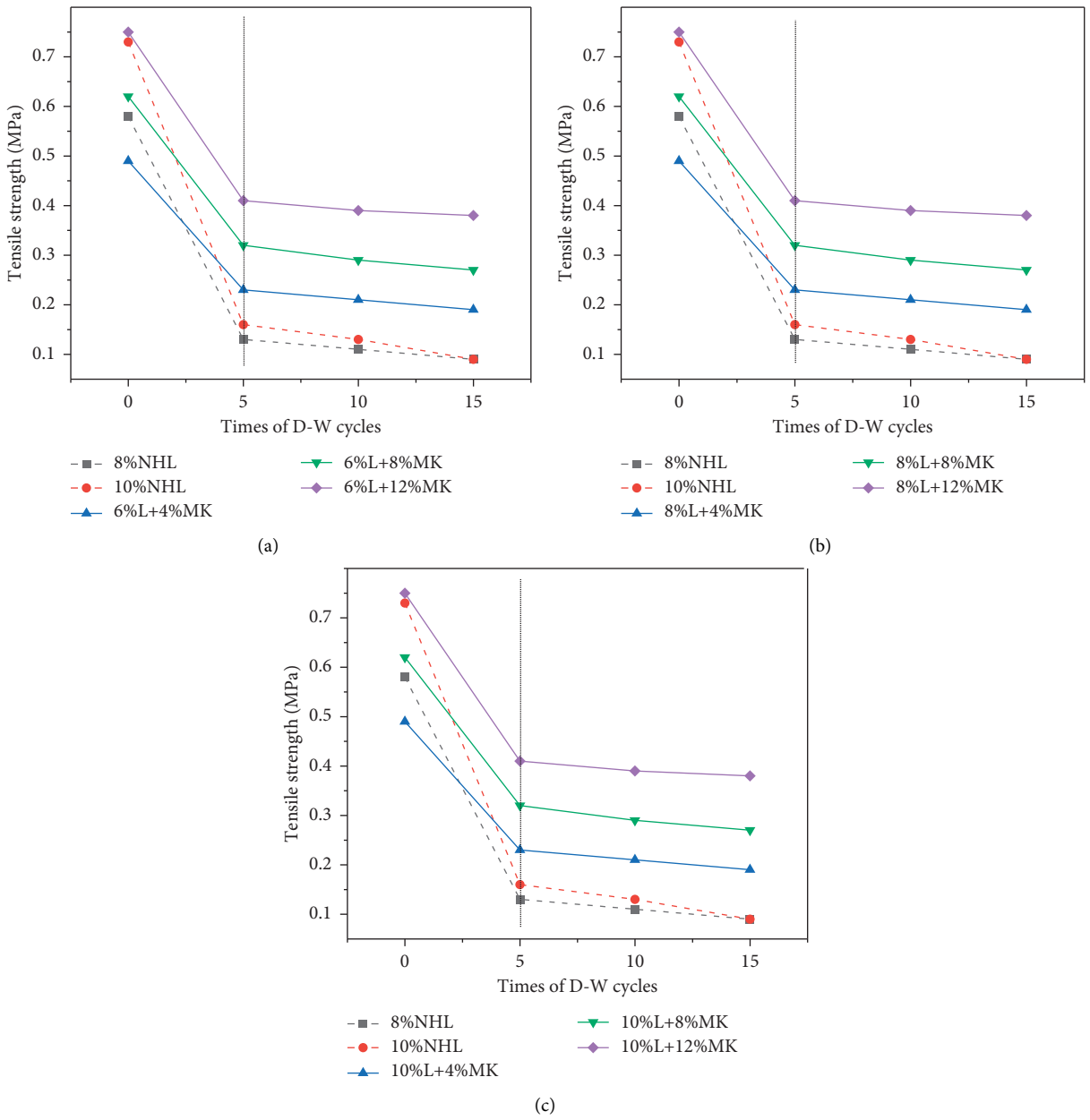

Figure 8: Relationship between the tensile strength of L-MK- and NHL-modified soils and the number of dry-wet cycles. (a) 6% L-MK and NHL. (b) 8% L-MK and NHL. (c) 10% L-MK and NHL.

reaction of lime to generate $Ca(OH)_2$, and $Ca(OH)_2$ ionized Ca^+, and OH^- will react with SiO_2 and Al_2O_3 in MK to generate CSH and C_4AH_{13}. The uninvolved SiO_2 and supersaturated $Ca(OH)_2$ remain in the crystalline state. The reaction equations are given by equations (1) and (2). In the above reaction products, the increasing CSH and $Ca(OH)_2$ contents improve the mechanical strength of the sample [29], and the CSH contribution strengthens with ageing and MK content. C_4AH_{13} is reduced or converted continuously into other hydration products over time [30].

$$Al_2O_3 \cdot 2SiO_2 + 3Ca(OH)_2 + 6H_2O \longrightarrow 2CaO \cdot Al_2O_3 \cdot SiO_2 \cdot 8H_2O + CaO - SiO_2 - H_2O \quad (1)$$

$$Al_2O_3 \cdot 2SiO_2 + 6Ca(OH)_2 + 9H_2O \longrightarrow 4CaO \cdot Al_2O_3 \cdot 13H_2O + 2CaO - SiO_2 - H_2O \quad (2)$$

Compared with the measurements of the L-MK-modified soil before any dry-wet cycles, it was found that the

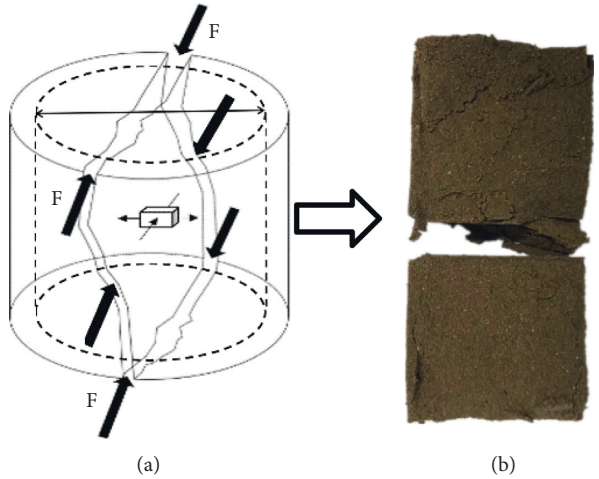

Figure 9: STS tensile failure mode and morphology. (a) Stress state. (b) Failure mode.

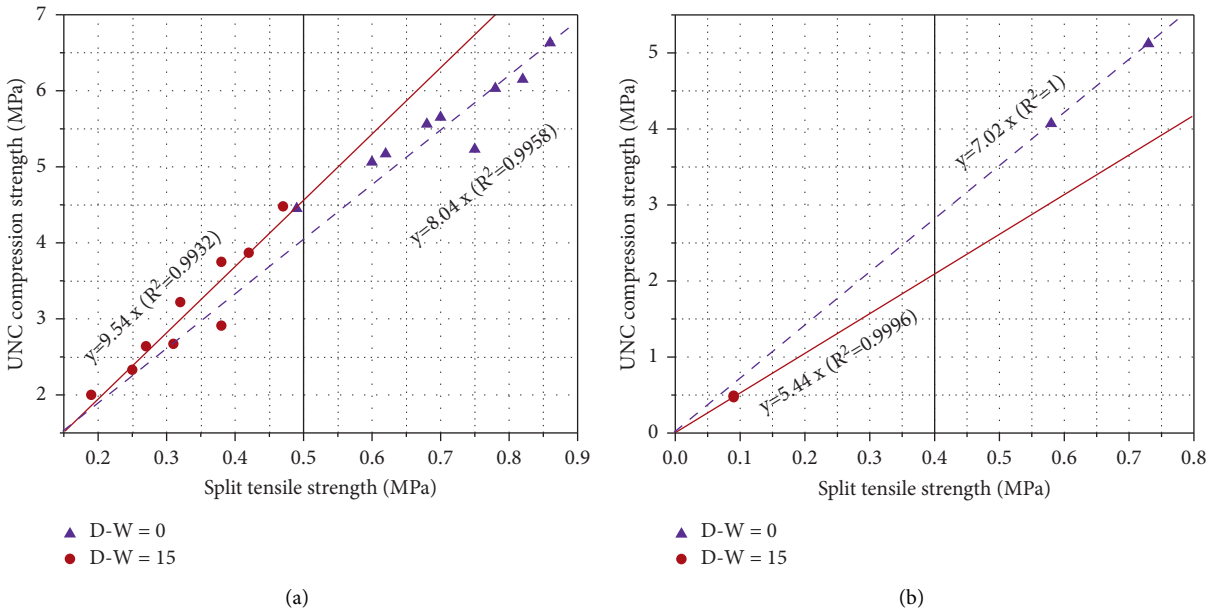

Figure 10: Relationship between the compressive and tensile strengths of the L-MK- and NHL-modified soil. (a) L-MK. (b) NHL.

relative strength of the characteristic peaks at 27.6° (main characteristic peak of CSH) and 29.4° (main characteristic peak of C_4AH_{13}) decreased after 15 dry-wet cycles, indicating that the contents of CSH and C_4AH_{13} decreased gradually. In the measurements of the NHL-modified soil, the relative strength of the characteristic peaks at 19.8° (main characteristic peak of $Ca(OH)_2$) and 27.6° (main characteristic peak of CSH) also decreased after 15 dry-wet cycles. The above results show that the decrease in hydration products after dry-wet cycles reduced the compactness of the soil structure and has a negative impact on its strength [29].

4.2. TG Test. Differential scanning (DSC) and TG analysis were performed on the L-MK- and NHL-modified soils, and the results are shown in Figure 12. Figure 12 shows that at the initial stage of heating, the curves showed large endothermic peaks and uniform weight loss, which was caused by the loss of adsorbed water in the initial stage and the removal of gel water and interlayer water in the form of water molecules after 100°C. In addition, the DSC curve for the L-MK-modified soil presented three endothermic peaks in three different temperature ranges, which is speculated to have been caused by the removal of structural water decomposition by C_4AH_{13} (162°C), $Ca(OH)_2$ (425°C), and CSH (747°C), with some C_4AH_{13} being decomposed into $Ca(OH)_2$ and $4CaO{\cdot}3Al_2O_3{\cdot}3H_2O$ [30, 31]. The contents of CSH, $Ca(OH)_2$, and C_4AH_{13} can be estimated according to the above temperature range of dehydration of the hydration products and the mass loss of the TG curve. The results are given in Table 3.

Table 3 shows that after 15 dry-wet cycles of soil modified by 8% L + 4% MK, the contents of CSH and C_4AH_{13} decreased from 1.67% and 0.91% to 0.58% and 0.65%,

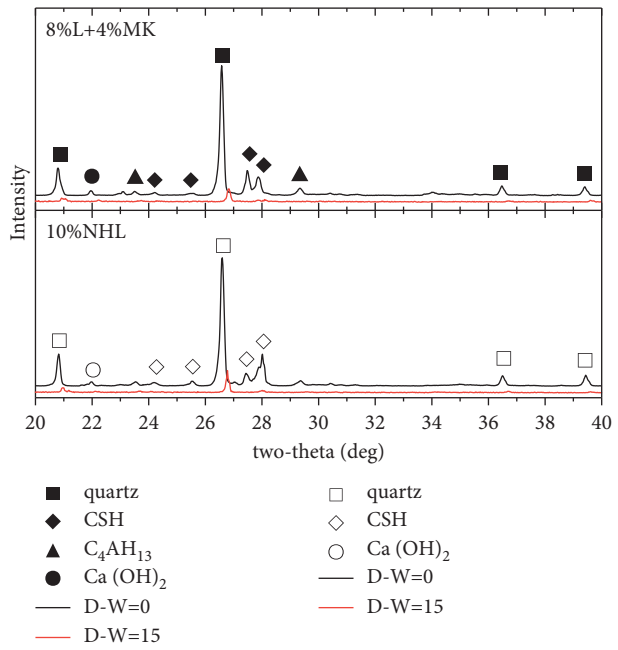

Figure 11: XRD results of hydration products of L-MK- and NHL-modified soils before and after dry-wet cycles (20°~40°).

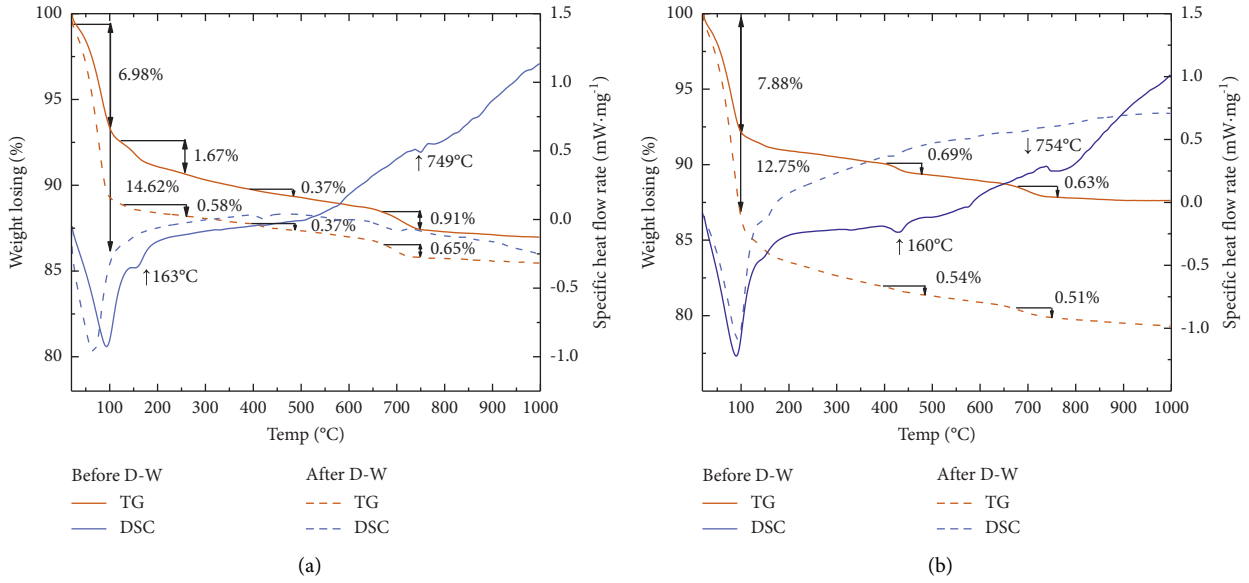

Figure 12: TG-DSC chart of 8% L + 4% MK and 10% NHL-modified soil before and after dry-wet cycle. (a) 8% L + 4% MK. (b) 10% NHL.

Table 3: Calculation results of CSH, Ca(OH)$_2$, and C_4AH_{13} contents.

Sample		Content of hydration products/%		
		C4AH13 (130–250°C)	Ca(OH)$_2$ (400–480°C)	CSH (680–750°C)
8% L+4% MK	Before D-W	1.67	0.37	0.91
	After D-W	0.58	0.37	0.65
10% NHL	Before D-W	—	0.69	0.63
	After D-W	—	0.54	0.51

respectively, but the content of Ca(OH)$_2$ did not change. It is speculated that Ca(OH)$_2$ decomposed by C_4AH_{13} filled part of Ca(OH)$_2$ that was affected by dry-wet cycles. The contents of Ca(OH)$_2$ and CSH in soil modified by 10% NHL decreased from 0.69% and 0.63% to 0.54% and 0.51%, respectively, under dry-wet cycles. The contents of CSH before

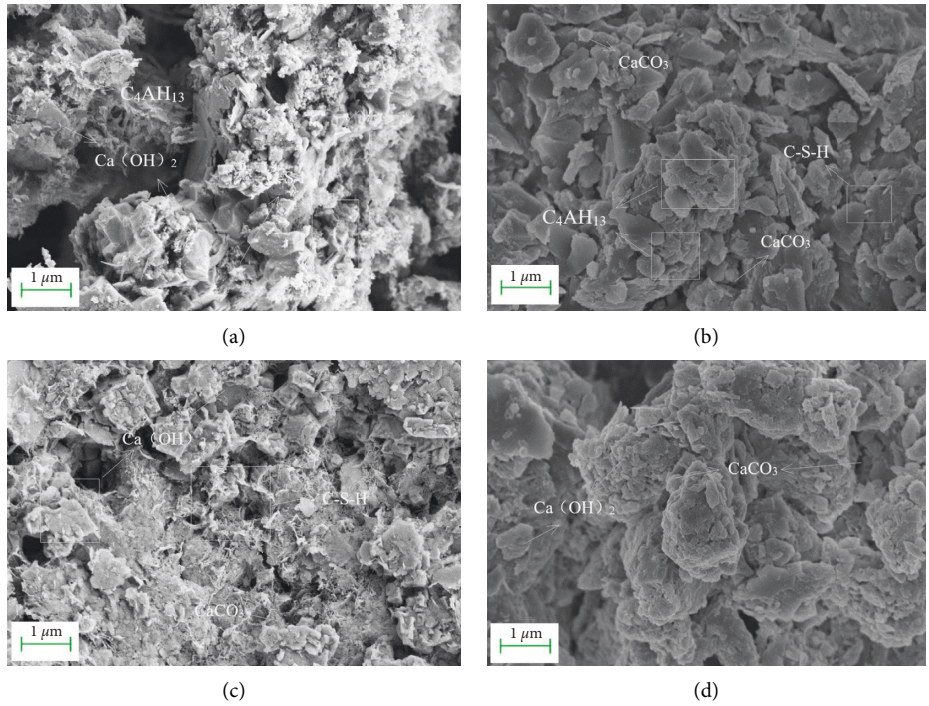

Figure 13: (a) L-MK before dry-wet cycle. (b) L-MK after dry-wet cycle. (c) NHL before dry-wet cycle. (d) NHL after dry-wet cycle.

and after dry-wet cycles were lower than those of L-MK-modified soil. This is consistent with the variation laws of compressive and tensile strengths in Sections 3.2 and 3.3 with the number of dry-wet cycles.

4.3. SEM Test. SEM was used to observe the microstructure of samples before any dry-wet cycles and after 15 dry-wet cycles. The results are shown in Figure 13.

Figure 13 shows the SEM images of L-MK- and NHL-modified soils before any dry-wet cycles and after 15 dry-wet cycles at a magnification of 10000. According to Figure 13(a) and the XRD results, the hydration products of the L-MK-modified soil before any dry-wet cycles were mainly laminar C_4AH_{13}, fibrous reticular CSH, and irregular lamellar $Ca(OH)_2$. CSH and C_4AH_{13} were distributed on the surface of $Ca(OH)_2$ or filled in structural pores and were interwoven with $Ca(OH)_2$ to form a relatively complete dense structure, imparting higher strength. Figure 13(b) shows that the interlocking structure between pozzolanic reaction products and $Ca(OH)_2$ in the L-MK-modified soil after 15 dry-wet cycles was reduced significantly, and the filling products between individual pores disappeared. In addition, a small amount of cubic $CaCO_3$ crystals was also observed, indicating that the soil had begun the carbonation process, and part of $Ca(OH)_2$ was decomposed into $CaCO_3$ crystals by carbonation reaction. Combined with the fact that the $Ca(OH)_2$ content of the L-MK-modified soil in Table 3 before and after 15 dry-wet cycles did not change, it can be concluded that the secondary pozzolanic reaction offsets the influence of the carbonation reaction and dry-wet cycles on the $Ca(OH)_2$ content.

Figures 13(c) and 13(d) show that the hydration products of the NHL- and L-MK-modified soils had different morphologies. $CaCO_3$ produced by carbonation was distributed on or filled the laminar $Ca(OH)_2$ and amorphous CSH gel that formed the main skeleton structure of the NHL-modified soil in a step-by-step manner. After 15 dry-wet cycles, the microstructure morphology of the samples also showed similar regular changes to those of the L-MK-modified soil, but the coverage area of the hydration products of the NHL-modified soil on soil particle aggregates was significantly lower than that of the L-MK-modified soil.

5. Conclusions

(1) The mass loss ratio of L-MK- and NHL-modified soil decreased by less than 2% after 15 dry-wet cycles meeting the requirement of the ASTM standard of 8%. The content of hydrates involved in the pozzolanic reaction increased gradually, and the cementation among soil particles strengthened with increasing MK content leading to decrease in the mass loss of the L-MK-modified soil samples.

(2) The peak strain ε_f and the corresponding peak compressive strength of the L-MK-modified soil decreased with more dry-wet cycles. After 15 dry-wet cycles, the compressive strength decreased by 32.43–55.06%, which was better than that of the NHL-modified soil (~89.39%), and the absolute value of the compressive strength of the L-MK-modified soil was between four and nine times that of the NHL-modified soil under the same dry-wet cycles.

(3) The tensile strength of the L-MK-modified soil decreased gradually with more dry-wet cycles and was higher than that of the NHL-modified soil. However, the difference was that the attenuation process for the tensile strength was a steep decrease initially followed by a slow decrease after five dry-wet cycles. The compressive strength had no obvious segmented attenuation process, which is related to the internal and external heterogeneity of dry-wet cycles in soil and the different failure modes of compressive and tensile strength.

(4) The hydration products such as CSH and C4AH13 generated by the pozzolanic reaction of lime and MK were interwoven with $Ca(OH)_2$ to form a complete dense structure. However, after 15 dry-wet cycles, the contents of CSH and C4AH13 decreased from 1.67% and 0.91% to 0.58% and 0.65%, respectively, which was consistent with the change law of the strength characteristics.

(5) Combining the test results for mechanical strength and the microscopic mechanism, it is feasible and effective to use lime together with MK as a restoration material for silty soil or silty sand sites, and 6% L + 4% MK can effectively replace 8% and 10% NHL for protecting soil sites from the perspective of dry and wet resistance.

Data Availability

The data used to support the findings of this study are available from the corresponding author upon request.

Conflicts of Interest

The authors declare that they have no conflicts of interest.

Acknowledgments

This work was supported by the Young Backbone Teachers Funding Program of Higher Education in Henan Province (grant nos. 2019GGJS142 and 2020GGJS136); Open Foundation of State Key Laboratory of Geomechanics and Geotechnical Engineering (grant no. Z0190202); Science and Technology Project of Henan Province (grant no. 202102310931); and The Basic Research Project of Henan Provincial Key Scientific Research Project (20ZX009).

References

[1] Q. Y. Zhang, W. W. Chen, and W. J. Fan, "Protecting earthen sites by soil hydrophobicity under freeze–thaw and dry–wet cycles," *J. Constr. Build. Mater.,* vol. 262, 2020.

[2] K. B. Ren, B. Wang, and X. M. Li, "Strength properties and pore-size distribution of earthen archaeological site under dry-wet cycles of capillary water," *J. Rock and Soil Mechanics*, vol. 40, no. 03, pp. 962–970, 2019.

[3] D. Q. Kong, J. Chen, R. Wan, and H. Liu, "Study on restoration materials for historical silty earthen sites based on lime and starch ether," *Advances in Materials Science and Engineering*, vol. 2020, Article ID 2850780, 16 pages, 2020.

[4] A. Moropoulou, A. Bakolas, and K. Bisbikou, "Investigation of the technology of historic mortars," *Journal of Cultural Heritage*, vol. 1, no. 1, pp. 45–58, 2000.

[5] A. Maria, B. Asterios, and K. Meletis, "Mechanical and physical performance of natural hydraulic lime mortars," *J. Constr. Build. Mater.,* vol. 290, 2021.

[6] A. Arizzi, H. Viles, and G. Cultrone, "Experimental testing of the durability of lime based mortars used for rendering historic buildings," *Construction and Building Materials*, vol. 28, no. 1, pp. 807–818, 2012.

[7] A. Moropoulou, A. Bakolas, P. Moundoulas, E. Aggelakopoulou, and S. Anagnostopoulou, "Strength development and lime reaction in mortars for repairing historic masonries," *Cement and Concrete Composites*, vol. 27, no. 2, pp. 289–294, 2005.

[8] P. Miller, M. Rabinowitz, and J. Sembrat, "The use and effectiveness of dispersed hydrated lime in conservation of monuments and historic structures," in *Proceedings of the C. International Building Lime Symposium 2005*, Orlando, Florida, March 2005.

[9] V. Alvarez and I. Pingarrón, *Performance Analysis of Hydraulic Lime Grouts for Masonry Repair*, D. University of Pennsylvania, Pennsylvania, 2006.

[10] G. Pesce, "Optimization of the thermal activation of kaolin used as hydraulic additive for air lime influence of partial pressure of water on the reactivity of metakaolin," *J. Febs Letters,* vol. 450, no. 1, pp. 84–88, 1999.

[11] B. Sabir, S. Wild, and J. Bai, "Metakaolin and calcined clays as pozzolans for concrete: a review," *Cement and Concrete Composites*, vol. 23, no. 6, pp. 441–454, 2001.

[12] V. Pavlik and M. Uzakova, "Effect of curing conditions on the properties of lime, lime–metakaolin and lime–zeolite mortars, Lime-metakaolin and Lime-zeolite Mortars," *Construction and Building Materials*, vol. 102, no. 1, pp. 14–25, 2016.

[13] M. W. Wang, K. Ge, and D. R. Zhu, "Experimental study of engineering behaviors on improved expansive soils in the xinqiao airport runway of hefei," *Advanced Materials Research*, vol. 261-263, pp. 1329–1335, 2011.

[14] N. C. Consoli, K. Da Silva, S. Filho, and A. B. Rivoire, "Compacted clay-industrial wastes blends: long term performance under extreme freeze-thaw and wet-dry conditions," *Applied Clay Science*, vol. 146, pp. 404–410, 2017.

[15] C. G. Yan, Z. Q. Zhang, and Y. L. Jing, "Characteristics of strength and pore distribution of lime-flyash loess under freeze-thaw cycles and dry-wet cycles," *Arabian Journal of Geosciences*, vol. 10, no. 24, 544 pages, 2017.

[16] A. Aldaood, M. Bouasker, and M. Al-Mukhtar, "Impact of wetting–drying cycles on the microstructure and mechanical properties of lime-stabilized gypseous soils," *Engineering Geology*, vol. 174, pp. 11–21, 2014.

[17] S. Pavía and E. Treacy, "A comparative study of the durability and behaviour of fat lime and feebly-hydraulic lime mortars," *Materials and Structures*, vol. 39, no. 3, pp. 391–398, 2006.

[18] Z. J. Song, Z. Y. Lu, and Z. Y. Lai, "Mechanical and durability performance improvement of natural hydraulic lime-based mortars by lithium silicate solution," *Materials*, vol. 13, no. 22, 5292 pages, 2020.

[19] A. Kalagri, A. Miltiadou-Fezans, and E. Vintzileou, "Design and evaluation of hydraulic lime grouts for the strengthening of stone masonry historic structures," *Materials and Structures*, vol. 43, no. 8, pp. 1135–1146, 2010.

[20] A. M. Forster and K. Carter, "A framework for specifying natural hydraulic lime mortars for masonry construction," *Structural Survey*, vol. 29, no. 5, pp. 373–396, 2011.
[21] A. Sepulcre Aguilar and F. Hernández-Olivares, "Interfacial transition zone (ITZ) analysis in hydraulic lime restoration mortars for grouting of historical masonries," *International Journal of Architectural Heritage*, vol. 6, no. 4, pp. 396–414, 2012.
[22] G. Banzibaganye, E. Twagirimana, and G. S. Kumaran, "Strength enhancement of silty sand soil subgrade of highway pavement using lime and fines from demolished concrete wastes," *International Journal of Engineering Research in Africa*, vol. 36, pp. 74–84, 2018.
[23] K. B. Ren, *Effects of Dry-Wet Cycle on silt Mechanical Properties of Guchengzhai and Response Characteristics of the wall*, D. Zhengzhou University, Zhengzhou, China, 2019.
[24] L. Q. Wang, "Temporal and spatial variation characteristics of extreme temperature in henan Province," *Open Journal of Nature Science*, vol. 07, no. 06, pp. 549–560, 2019.
[25] Fhwa, "Soil and base stabilization and associated drainage considerations," *Federal Highway*, vol. 1, 1993.
[26] N. C. Consoli, R. A. Quinonez Samaniego, L. E. Gonzalez, E. J. Bittar, and O. Cuisinier, "Impact of severe climate conditions on loss of mass, strength, and stiffness of compacted fine-grained soils–portland cement blends," *Journal of Materials in Civil Engineering*, vol. 30, no. 8, 2018.
[27] J. Cabrera and M. F. Rojas, "Mechanism of hydration of the metakaolin–lime–water system," *Cement and Concrete Research*, vol. 31, no. 2, pp. 177–182, 2001.
[28] X. M. Li, S. Yin, and J. C. Le, "Study on dry-wet cycle deterioration effect and mechanism of strength of steel slag-doped soil," *J. HIGHWAY*, vol. 62, no. 05, pp. 199–204, 2017.
[29] A. S. Silva, A. Gameiro, J. Grilo, R. Veiga, and A. Velosa, "Long-term behavior of lime-metakaolin pastes at ambient temperature and humid curing condition," *Applied Clay Science*, vol. 88-89, no. 3, pp. 49–55, 2014.
[30] P. De Silva and F. Glasser, "Phase relations in the system CaO-Al_2O_3-SiO_2-H_2O relevant to metakaolin-calcium hydroxide hydration," *Cement and Concrete Research*, vol. 23, no. 3, pp. 627–639, 1993.
[31] A. Gameiro, A. Santos Silva, P. Faria et al., "Physical and chemical assessment of lime-metakaolin mortars: influence of binder: aggregate ratio," *Cement and Concrete Composites*, vol. 45, no. 45, pp. 264–271, 2014.